VOL. 14, NO. 4, FEBRUARY 2019 ISSN 1819-6608
ARPN Journal of Engineering and Applied Sciences

www.arpnjournals.com

EFFECTS OF UNIFORM AND NON UNIFORM SALINITY GRADIENTS ON THE ONSET OF DOUBLE DIFFUSIVE CONVECTION IN A COMPOSITE LAYER: AN ANALYTICAL STUDY

B. Komala[1] and R. Sumithra[2]
[1]Development Centre, Bharathiar University, Coimbatore, Tamil Nadu, India
[1]B.T.L Institute of Technology and Management, Bommasandra, Bangalore, India
[2]Department of Mathematics, Government Science College, Bangalore, Karnataka, India
E-Mail: komala550@gmail.com,

ABSTRACT

The effects of Uniform and Non uniform salinity gradients on the onset of Double Diffusive Convection in a composite layer, comprising an incompressible two component fluid saturated porous layer over which lies a layer of the same fluid are investigated. The upper boundary of the fluid layer and the lower boundary of the porous layer are rigid and both the boundaries are insulating to heat and mass. At the interface, the velocity, shear stress, normal stress, heat, heat flux, mass and mass flux are assumed to be continuous conducive for Darcy-Brinkman model. The resulting Eigen value problem is solved by Regular perturbation method. The critical Rayleigh number for all the profiles is obtained and the effects of different physical parameter on the onset of double diffusive convection are investigated for all profiles. It is found that for the stability demanding situations like solar ponds, the parabolic salinity profile is the most conducive where in the onset of double diffusive convection in a composite layer can be delayed. For the heat and mass (solute or salt) transfer problems like petroleum and geothermal reservoirs, the inverted parabolic salinity profile is most suitable, where in the onset of double diffusive convection is fast.

Keywords: double diffusive convection, salinity gradients, darcy - brinkman model, solar pond.

1. INTRODUCTION

The sun is the largest source of all renewable energies on the earth and this energy is abundantly available in all parts of the earth. It is in fact one of the best alternatives to the non-renewable sources of energy. One way to tap solar energy is through the use of solar ponds. Solar ponds are large-scale energy collectors with integral heat storage for supplying thermal energy for process heating, water desalination, refrigeration, drying and power generation. The solar pond works on a very simple principle well-known that water or air is heated they become lighter and rise upward e.g. a hot air balloon. Similarly, in an ordinary pond, the sun's rays heat the water and the heated water within the pond rises and reaches the top but loses the heat into the atmosphere. The net result is that the pond water remains at the atmospheric temperature. The solar pond restricts this tendency by dissolving salt in the bottom layer of the pond making it too heavy to rise. A solar pond has three zones. The top zone is the surface zone, or UCZ (Upper Convective Zone), which is at atmospheric temperature and has little salt content. The bottom zone is very hot, 70°– 85° C, and is very salty. It is this zone that collects and stores solar energy in the form of heat, and is, therefore, known as the storage zone or LCZ (Lower Convective Zone). Separating these two zones is the important gradient zone or NCZ (Non-Convective Zone). Here the salt content increases as depth increases, thereby creating a salinity or density gradient. If we consider a particular layer in this zone, water of that layer cannot rise, as the layer of water above has less salt content and is, therefore, lighter. Similarly, the water from this layer cannot fall as the water layer below has a higher salt content and is, therefore, heavier. This gradient zone acts as a transparent insulator permitting sunlight to reach the bottom zone but also entrapping it there. The trapped (solar) energy is then withdrawn from the pond in the form of hot brine from the storage zone.

In the situation explained above, the occurrence of non-uniform gradients of salinity and temperature is a reality. With reference to the above application in mind we are investigating the onset of Double diffusive (thermo haline) convection in a Composite layer (two layer) comprising of an incompressible two component (temperature and salt) fluid saturated porous layer over which lies a layer of the same fluid. This composite layer is subjected to different salinity gradients in search of the most stable gradient suitable for the solar pond. The upper boundary of the fluid layer and the lower boundary of the porous layer are rigid and are insulating to heat and salt. At the interface, the velocity, shear stress, normal stress, heat and heat flux, salt and salt flux are assumed to be continuous conducive for Darcy-Brinkman model. The Eigen value of the problem, the critical Rayleigh number is obtained for all the salinity gradients. The effects of the various physical parameters on the stability of the system are investigated in detail. The problem also finds applications in petroleum and geothermal reservoirs, underground spreading of fertilizers, growth of crystals (isothermal and non - isothermal methods), solidification of alloys, materials processing and many more. In these situations, presence of non-uniform salinity gradients is a reality but the fundamental research in this area is to be focused.

Recently Pranesh *et al* [1] have investigated the effect of non uniform basic concentration gradient on the

onset of double diffusive convection in a micro polar fluid layer heated and soluted from below and cooled from above, using Galerkin method for different velocity boundary combinations with isothermal on spin-vanishing permeable boundaries. They have observed that the fluid layer with suspended particles heated and soluted from below is more stable compared to the classical fluid layer without suspended particles.

Ray-Yeng Yang *et al* [2] have investigated the overstability analysis on salt-fingers convection with parabolic temperature and salinity profiles. They explored the influence of parabolic profiles of temperature and salinity, as might arise due to local evaporation or warming disturbance, on the marginal stability problem in a salt fingering regime. They have also investigated the Marginal stability analysis on salt-fingers convection with parabolic temperature and salinity profiles.

Giestas *et al* [3] presented a 2D numerical model where the behavior of a salt gradient solar pond (SGSP) is described in terms of temperature, salt concentration and velocity with the fluid density and viscosity dependent on temperature and salt concentration. The discretization of the governing equations is based on the respective weak formulations. The rectangular geometry allows for spectral type Galerkin approximations for with the essential homogeneous boundary conditions can easily be imposed. Taking into the account the variation of density and viscosity with temperature and salinity improved the agreement between the numerical and the experimental results.

2. FORMULATION OF THE PROBLEM

We consider a horizontal two - component fluid saturated, isotropic, sparsely packed porous layer of thickness d_m underlying a two component fluid layer of thickness d .The lower surface of the porous layer and the upper surface of the fluid layer are rigid and are insulating to heat and mass. A Cartesian coordinate system is chosen with the origin at the interface between porous and fluid layers and the z - axis, vertically upwards. The basic steady state is assumed to be the quiescent and the governing equations are continuity, momentum, energy and concentration equations with Boussinesq approximation.

For fluid layer

$$\nabla \cdot \vec{q} = 0 \tag{1}$$

$$\rho_0 \left[\frac{\partial \vec{q}}{\partial t} + (\vec{q} \cdot \nabla)\vec{q} \right] = -\nabla P + \mu \nabla^2 \vec{q} - \rho g \hat{k} \tag{2}$$

$$\frac{\partial T}{\partial t} + (\vec{q} \cdot \nabla) T = \kappa \nabla^2 T \tag{3}$$

$$\frac{\partial C}{\partial t} + (\vec{q} \cdot \nabla) C = \kappa_s \nabla^2 C \tag{4}$$

And the state equation is $\rho = \rho_0 \left[1 - \alpha_t (T - T_0) + \alpha_s (C - C_0) \right]$

For the porous layer,

$$\nabla_m \cdot \vec{q}_m = 0 \tag{5}$$

$$\rho_0 \left(\frac{1}{\phi} \left(\frac{\partial \vec{q}_m}{\partial t} \right) + \frac{1}{\phi^2} (\vec{q}.\nabla)\vec{q} \right) = -\nabla_m P_m + \mu_m \nabla^2 \vec{q}_m - \frac{\mu}{K} \vec{q}_m - \rho_m g \hat{k} \tag{6}$$

$$A \frac{\partial T_m}{\partial t} + (\vec{q}_m \cdot \nabla_m) T_m = \kappa_m \nabla_m^2 T_m \tag{7}$$

$$\phi \frac{\partial C_m}{\partial t} + (\vec{q}_m.\nabla) C_m = \kappa_{sm} \nabla^2 C_m \tag{8}$$

and the state equation is $\rho_m = \rho_0 \left[1 - \alpha_t (T_m - T_0) + \alpha_s (C_m - C_0) \right]$

where $\vec{q} = (u, v, w)$ is the velocity vector, ρ_0 is the constant fluid density, t is the time, P is fluid pressure, μ is the fluid viscosity, ρ is the fluid density , g is the acceleration due to gravity, $A = \frac{(\rho_0 C_p)_m}{(\rho C_p)_f}$ is the ratio of heat capacities, C_p is the specific heat, K is the permeability of the porous medium, T is the temperature, κ is the thermal diffusivity of the fluid, C is the concentration/solute/salt, κ_s is the solute diffusivity of the fluid, ϕ is the porosity, α_t is the thermal expansion coefficient, α_s is the Concentration/solute expansion coefficient and the subscripts m and f refer to the porous medium and the fluid respectively.

In order to investigate the stability of the basic solution, infinitesimal disturbances are introduced. Equations (1) to (8) are linearized and the pressure term is eliminated from (2) and (6) by taking curl twice on those two equations and only the vertical component is retained. The variables are then non-dimensionalised using $\frac{d^2}{\kappa}$, $\frac{\kappa_m}{d_m}$, $T_0 - T_u$ and $C_0 - C_u$ as the units of time velocity, temperature, and the concentration in the fluid

layer and $\frac{d_m^2}{\kappa_m}$, $\frac{\kappa_m}{d_m}$, $T_l - T_0,$, $C_l - C_0$ as the corresponding characteristic quantities in the porous layer. The separate length scales are chosen for the two layers (Chen and Chen [4], D.A Nield [5]), so that each layer is of unit depth with $(x, y, z) = d(x', y', z')$ & $(x_m, y_m, z_m) = d_m(x'_m, y'_m, z'_m - 1)$. In this manner the detailed flow fields in both the fluid and porous layers can be clearly obtained for all the depth ratios $\hat{d} = \frac{d_m}{d}$. The non dimensionalised basic equations are subjected to normal mode expansion and seek solutions for the dependent variables in the fluid and porous layers (following Venkatachalappa M *et al* [6]). It is known that the principle of exchange of instabilities holds for Double Diffusive convection in both fluid and porous layers separately for certain choice of parameters. Therefore, we assume that the principle of exchange of instabilities holds even for the composite layers (following Nield [5]).

Denoting the differential operator $\frac{\partial}{\partial z}$ and $\frac{\partial}{\partial z_m}$ by D and D_m respectively, an Eigen value problem consisting of the following ordinary differential equations is obtained,

In $0 \le z \le 1$,

$$\left(D^2 - a^2\right)^2 W(z) = Ra^2\Theta - R_s a^2 S \tag{9}$$

$$\left(D^2 - a^2\right)\Theta(z) + W(z) = 0 \tag{10}$$

$$\tau\left(D^2 - a^2\right)S(z) + W(z)\, h(z) = 0 \tag{11}$$

In $0 \le z_m \le 1$

$$\left[\left(D_m^2 - a_m^2\right)\hat{\mu}\beta^2 - 1\right]\left(D_m^2 - a_m^2\right)W_m(z_m) = R_m a_m^2 \Theta_m - R_{sm} a_m^2 S_m \tag{12}$$

$$\left(D_m^2 - a_m^2\right)\Theta_m(z_m) + W_m(z_m) = 0 \tag{13}$$

$$\tau_m\left(D_m^2 - a_m^2\right)S_m(z_m) + W_m(z_m)\, h_m(z_m) = 0 \tag{14}$$

where $R = \frac{g\alpha_t\left(T_0 - T_u\right)d^3}{\nu\kappa}$ is the thermal Rayleigh number, $R_s = \frac{g\alpha_s\left(C_0 - C_u\right)d^3}{\nu\kappa}$ is the solute Rayleigh number in the fluid layer $\tau = \frac{\kappa_s}{\kappa}$ is the solutal-thermal diffusivity ratio, $\beta^2 = \frac{K}{d_m^2} = Da$ is the Darcy number, $\hat{\mu} = \frac{\nu_m}{\nu}$ is the viscosity ratio, $\tau_m = \frac{\kappa_{sm}}{\kappa_m}$ is solutal-thermal diffusivity ratio, $R_m = \frac{g\alpha_t\left(T_L - T_0\right)\kappa d_m}{\nu\kappa_m}$ is the thermal Rayleigh number, $R_{sm} = \frac{g\alpha_s\left(C_L - C_0\right)\kappa d_m}{\nu\kappa_m}$ is the solute Rayleigh number, a and a_m are the non-dimensional horizontal wave numbers, Θ and Θ_m are the temperature in fluid and porous layers, S and S_m are the concentration in fluid and porous layers, and $\int_0^1 h(z)\, dz = 1$ and $\int_0^1 h_m(z_m)\, dz_m = 1$.

Thus we have sixteenth order ordinary differential equation and which needs sixteen boundary conditions.

3. BOUNDARY CONDITIONS

The Sixteen boundary conditions after non-dimensionalised and Normal mode expansion and are given by

$$\begin{aligned}
&W(1) = 0, \quad DW(1) = 0, \quad D\Theta(1) = 0, \quad DS(1) = 0,\\
&w_m(0) = 0, \quad D_m w_m(0) = 0, \quad D_m\Theta_m(0) = 0, \quad D_m S_m(0) = 0,\\
&\hat{T}W(0) = W_m(1), \quad \hat{T}\hat{d}DW(0) = D_m W_m(1), \quad \Theta(0) = \hat{T}\Theta_m(1),\\
&\hat{T}\hat{d}^2\left(D^2 + a^2\right)W(0) = \hat{\mu}\left(D_m^2 + a_m^2\right)W_m(1), \quad D\Theta(0) = D_m\Theta_m(1),\\
&\hat{T}\hat{d}^3\beta^2\left(D^3W(0) - 3a^2DW(0)\right) = -D_m W_m(1) + \hat{\mu}\beta^2 D_m^3 W_m(1) -\\
&\hat{\mu}\beta^2 3a_m^2 D_m W_m(1), \quad S(0) = \hat{S}S_m(1), \quad DS(0) = D_m S_m(1).
\end{aligned} \tag{15}$$

Where $\hat{T} = \left(T_L - T_0\right)/\left(T_0 - T_U\right)$, $\hat{S} = \left(C_L - C_0\right)/\left(C_0 - C_U\right)$, and $\hat{d} = d_m/d$ is the depth ratio. We see that $\hat{\kappa} = \kappa_m/\kappa = \hat{d}/\hat{T}$ and $\hat{\kappa}_s = \kappa_{sm}/\kappa_s = \hat{d}/\hat{S}$ because the steady state heat and mass fluxes are continuous across the interface where $\hat{\kappa}$

and $\hat{\kappa}_s$ are the thermal diffusivity and the solutal diffusivity ratios respectively. The Energy Equations are solved using respective boundary conditions from (15) (following Shivakumara I.S *et al* [7]).

4. SOLUTION BY REGULAR PERTURBATION TECHNIQUE

For the constant heat and mass flux boundaries, convection sets in at small values of horizontal wave number 'a', accordingly, we expand

$$\begin{bmatrix} W \\ \theta \\ S \end{bmatrix} = \sum_{j=0}^{\infty} a^{2j} \begin{bmatrix} W_j \\ \Theta_j \\ S_j \end{bmatrix} \text{And} \begin{bmatrix} w_m \\ \theta_m \\ S_m \end{bmatrix} = \sum_{j=0}^{\infty} \left(\hat{d}a\right)^{2j} \begin{bmatrix} W_{mj} \\ \theta_{mj} \\ S_{mj} \end{bmatrix}$$

The equations at first order in a^2 are

In $0 \le z \le 1$

$$D^4 W_1 - R\hat{T} + R_s \hat{S} = 0 \tag{16}$$

$$D^2 \Theta_1 - \hat{T} + W_1 = 0 \tag{17}$$

$$\tau D^2 S_1 - \tau \hat{S} + W_1 h(z) = 0 \tag{18}$$

and in $0 \le z_m \le 1$

$$\hat{\mu}\beta^2 D_m^4 W_{m1} - D_m^2 W_{m1} - R_m + R_{sm} = 0 \tag{19}$$

$$D_m^2 \Theta_{m1} - 1 + W_{m1} = 0 \tag{20}$$

$$\tau_m D_m^2 S_{m1} - \tau_m + W_{m1} h_m(z_m) = 0 \tag{21}$$

The corresponding boundary conditions are

$$\begin{aligned}
&W_1(1) = 0, \quad DW_1(1) = 0, \quad D\Theta_1(1) = 0, \quad DS_1(1) = 0 \\
&\hat{T}W_1(0) = \hat{d}^2 W_{m1}(1), \quad \hat{T}DW_1(0) = \hat{d}D_m W_{m1}(1), \\
&\hat{T}D^2 W_1(0) = \hat{\mu}D_m^2 W_{m1}(1), \quad \theta_1(0) = \hat{T}\hat{d}^2 \theta_{m1}(1), \\
&\hat{T}\hat{d}\beta^2 D^3 W_1(0) = -D_m W_{m1}(1) + \hat{\mu}\beta^2 D_m^3 W_{m1}(1), \\
&D\theta_1(0) = \hat{d}^2 D_m \theta_{m1}(1), \quad S_1(0) = \hat{S}\hat{d}^2 S_{m1}(1), \\
&DS_1(0) = \hat{d}^2 D_m S_{m1}(1), \quad W_{m1}(0) = 0, \quad D_m W_{m1}(0) = 0, \\
&D_m \theta_{m1}(0) = 0, \quad D_m S_{m1}(1) = 0.
\end{aligned} \tag{22}$$

The solutions of the Equations. (16) and (19) give W_1 and W_{m1} respectively which are important in obtaining the Eigen values and they are found to be

$$W_1 = \frac{R\hat{T} - R_s \hat{S}}{24}\left(z^4 + C_4 z^3 + C_3 z^2 + C_2 z + C_1\right) \tag{23}$$

and

$$W_{m1} = C_5 + C_6 z_m + C_7 e^{pz_m} + C_8 e^{-pz_m} + \left(R_{ms} - R_m\right)\frac{z_m^2}{2} + \frac{R_{ms} - R_m}{p^2} \tag{24}$$

where $p = \sqrt{\dfrac{1}{\hat{\mu}\beta^2}}$ and $C_i's\left(i = 1,2,3,...,7\right)$ are arbitrary constants given by

$$C_1=\frac{24\hat{d}^2\left(C_7\left(-pe^{-p}-e^{-p}+1\right)+C_8e^{-p}\left(-1+p+e^{-p}\right)\right)}{\hat{T}\left(R\hat{T}-R_s\hat{S}\right)e^{-p}}+\frac{24\hat{d}^2e^{-p}\left(R_{ms}-R_m\right)}{2\hat{T}\left(R\hat{T}-R_s\hat{S}\right)e^{-p}},$$

$$C_2=\frac{24\hat{d}\left(C_7p\left(1-e^{-p}\right)+C_8e^{-p}p\left(1-e^{-p}\right)+\left(R_{ms}-R_m\right)e^{-p}\right)}{\hat{T}\left(R\hat{T}-R_s\hat{S}\right)e^{-p}},$$

$$C_3=\frac{12\hat{\mu}}{\hat{T}\left(R\hat{T}-R_s\hat{S}\right)e^{-p}}\left[C_7p^2+C_8e^{-2p}p^2+\left(R_{ms}-R_m\right)e^{-p}\right]$$

$$C_4=\frac{4\left(C_7p\left(e^{-p}+p-1\right)+C_8pe^{-2p}\left(1-p-e^{p}\right)\right)}{\hat{T}\hat{d}\beta^2\left(R\hat{T}-R_s\hat{S}\right)e^{-p}}-\frac{4\left(e^{-p}\left(R_{ms}-R_m\right)\right)}{\hat{T}\hat{d}\beta^2\left(R\hat{T}-R_s\hat{S}\right)e^{-p}},$$

$$C_5=-C_7-C_8-\frac{R_{sm}-R_m}{p^2},\quad C_6=-pC_7+pC_8$$

$$C_7=\frac{e^{-p}\hat{T}\left(R\hat{T}-R_s\hat{S}\right)\left(b_2-4a_2\right)+\left(R_{sm}-R_m\right)\left(a_3b_2-a_2b_3\right)}{\left(a_2b_1-a_1b_2\right)}$$

$$C_8=\frac{e^{-p}\hat{T}\left(R\hat{T}-R_s\hat{S}\right)\left(4a_1-b_1\right)+\left(R_{sm}-R_m\right)\left(a_1b_3-a_3b_1\right)}{\left(a_2b_1-a_1b_2\right)}$$

$$a_1=24\hat{d}^2\left(1-pe^{-p}-e^{-p}\right)+24\hat{d}p\left(1-e^{-p}\right)+12\hat{\mu}p^2+\frac{4p\left(-1+p+e^{-p}\right)}{\hat{d}\beta^2}$$

$$a_2=24\hat{d}^2\left(-1+p+e^{-p}\right)e^{-p}+24\hat{d}pe^{-p}\left(1-e^{-p}\right)+12\hat{\mu}p^2e^{-2p}+$$

$$\frac{4pe^{-2p}\left(1-p-e^{p}\right)}{\hat{d}\beta^2},\quad a_3=\left(12\hat{d}^2+24\hat{d}+12\hat{\mu}-\frac{4}{\hat{d}\beta^2}\right)e^{-p},$$

$$b_1=24\hat{\mu}p^2+24\hat{d}p\left(1-e^{-p}\right)+\frac{12p\left(-1+p+e^{-p}\right)}{\hat{d}\beta^2},\quad b_2=24\hat{d}pe^{-p}\left(1-e^{-p}\right)$$

$$+24\hat{\mu}p^2e^{-2p}+\frac{12pe^{-2p}\left(1-p-e^{p}\right)}{\hat{d}\beta^2},\quad b_3=\left(24\hat{d}+24\hat{\mu}-\frac{12}{\hat{d}\beta^2}\right)e^{-p}$$

4.1 Compatibility condition

The boundary conditions involving $D\theta_1, DS_1, D\theta_{m1}, DS_{m1}$ (23)$_{3,\,4,\,15\text{ and }16}$ and the differential equations involving $D^2\theta_1, D^2S_1, D^2\theta_{m1}, D^2S_{m1}$, yield the compatibility condition

$$\int_0^1 W_1dz+\tau_{pm}\int_0^1 W_1h(z)\,dz+\hat{d}^2\int_0^1 W_{m1}dz_m+\tau\hat{d}^2\int_0^1 W_{m1}h_m(z_m)\,dz_m=\left(\hat{s}+\hat{d}^2\right)\tau\tau_{pm}+\hat{T}+\hat{d}^2 \tag{25}$$

Thus, by substituting expressions for W_1 and W_{m1} in equation (25) we obtain an expression for critical Rayleigh number for different basic salinity profiles in both fluid and porous layers. The results thus obtained are discussed below.

4.2 Linear salinity profile

For this $h(z)=h_m(z_m)=1$. The critical Rayleigh number R_{c1} for this profile is obtained from (26) and is solved from the equation $\left(R_{c1}\hat{t}-R_s\hat{s}\right)B_1+\left(R_{sm}-R_m\right)B_2-\left(\hat{S}+\hat{d}^2\right)\tau\tau_m\Delta-\left(\hat{T}+\hat{d}^2\right)=0$

where

$$B_1=\frac{1+\tau_m}{120}+\frac{A_1\hat{t}e^{-p}\left(b_2-4a_2\right)+A_2\hat{t}e^{-p}\left(4a_1-b_1\right)}{a_2b_1-a_1b_2},$$

$$B_2=\frac{A_1\left(a_3b_2-a_2b_3\right)+A_2\left(a_1b_3-a_3b_1\right)}{\left(a_2b_1-a_1b_2\right)}+A_3,$$

$$A_1=\frac{\left(1+\tau_m\right)p\left(e^{-p}+p-1\right)}{24\hat{t}\hat{d}\beta^2e^{-p}}+\frac{\left(1+\tau_m\right)\hat{\mu}p^2}{6\hat{t}e^{-p}}+\frac{\left(1+\tau_m\right)\hat{d}p\left(1-e^{-p}\right)}{2\hat{t}e^{-p}}+$$

$$\frac{\left(1+\tau_m\right)\hat{d}^2\left(1-pe^{-p}-e^{-p}\right)}{\hat{t}e^{-p}}-\hat{d}^2\left(\frac{\left(1+\tau\right)\left(e^p-1\right)}{p}-\left(1+\tau\right)-\frac{\left(1+\tau\right)p}{2}\right),$$

$$A_2=\frac{\left(1+\tau_m\right)p\left(-e^{-p}-p+1\right)}{24\hat{t}\hat{d}\beta^2}+\frac{\left(1+\tau_m\right)\hat{\mu}p^2e^{-p}}{6\hat{t}}+\frac{\left(1+\tau_m\right)\hat{d}p\left(1-e^{-p}\right)}{2\hat{t}}$$

$$+\frac{\left(1+\tau_m\right)\hat{d}^2\left(-1+p+e^{-p}\right)}{\hat{t}}-\frac{\hat{d}^2\left(1+\tau\right)\left(e^{-p}-1\right)}{p}-\hat{d}^2\left(\left(1+\tau\right)+\frac{\left(1+\tau\right)p}{2}\right),$$

$$A_3=\frac{-\left(1+\tau_m\right)}{24\hat{t}\hat{d}\beta^2}+\frac{\left(1+\tau_m\right)\hat{\mu}}{6\hat{t}}+\frac{\left(1+\tau_m\right)\hat{d}}{2\hat{t}}+\frac{\left(1+\tau_m\right)\hat{d}^2}{\hat{t}}+\frac{1}{6},$$

and the constants $a_i^{'s}$ and $b_i^{'s}$ are defined previously.

4.3 Parabolic salinity profile

Following Sparrow *et al* [8], $h\left(z\right)=2z,\quad h_m\left(z_m\right)=2z_m$. The critical Rayleigh number R_{c2} for this profile is obtained from (26) and is solved from the equation

$$\left(R_{c2}\hat{t}-R_s\hat{s}\right)B_1+\left(R_{sm}-R_m\right)B_2-\left(\hat{S}+\hat{d}^2\right)\tau\tau_m\Delta-\left(\hat{T}+\hat{d}^2\right)=0$$

where

$$B_1=\frac{3+5\tau_m}{360}+\frac{A_1\hat{t}e^{-p}\left(b_2-4a_2\right)+A_2\hat{t}e^{-p}\left(4a_1-b_1\right)}{a_2b_1-a_1b_2},$$

$$B_2=\frac{A_1\left(a_3b_2-a_2b_3\right)+A_2\left(a_1b_3-a_3b_1\right)}{\left(a_2b_1-a_1b_2\right)}+A_3,$$

$$A_1=\frac{\left(5+8\tau_m\right)p\left(e^{-p}+p-1\right)}{120\hat{t}\hat{d}\beta^2e^{-p}}+\frac{\left(3+4\tau_m\right)\hat{d}p\left(1-e^{-p}\right)}{6\hat{t}e^{-p}}+\frac{\left(1+\tau_m\right)\hat{d}^2\left(1-pe^{-p}-e^{-p}\right)}{\hat{t}e^{-p}}+A_4,$$

$$A_4=\frac{\left(2+3\tau_m\right)\hat{\mu}p^2}{12\hat{t}e^{-p}}+\hat{d}^2\left(\frac{-2-p}{2}+\frac{\left(e^p-1\right)}{p}\right)+2\tau\hat{d}^2\left(\frac{-6-2p}{12}+\frac{\left(e^p-p-1\right)}{p^2}\right),$$

$$A_2=\frac{\left(5+8\tau_m\right)pe^{-p}\left(-e^p-p+1\right)}{120\hat{t}\hat{d}\beta^2}+\frac{\left(3+4\tau_m\right)\hat{d}p\left(1-e^{-p}\right)}{6\hat{t}}+\frac{\left(1+\tau_m\right)\hat{d}^2\left(-1+p+e^{-p}\right)}{\hat{t}}+A_5,$$

$$A_5=\frac{\left(2+3\tau_m\right)\hat{\mu}p^2e^{-p}}{12\hat{t}}+d^2\left(-1+\frac{p}{2}-\frac{\left(e^{-p}-1\right)}{p}+A_6\right),$$

$$\mathrm{A}_6=2\tau\hat{d}^2\left(\frac{3+2p}{6}+\frac{\left(-e^p-pe^{-p}+1\right)}{p^2}\right),$$

$$A_3=\frac{-\left(5+8\tau_m\right)}{120\hat{t}\hat{d}\beta^2}+\frac{\left(2+3\tau_m\right)\hat{\mu}}{12\hat{t}}+\frac{\left(3+4\tau_m\right)\hat{d}}{6\hat{t}}+\frac{\left(1+\tau_m\right)\hat{d}^2}{2\hat{t}}+d^2\left(\frac{1}{6}+\frac{\tau}{4}\right)$$

and the constants $a_i^{'s}$ and $b_i^{'s}$ are defined previously.

4.4 Inverted parabolic salinity profile

For this case, $h(z)=2(1-z)$, $h_m(z_m)=2(1-z_m)$. The critical Rayleigh number R_{c3} for this profile is obtained from (26) and is solved from the equation $\left(R_{c3}\hat{t}-R_s\hat{s}\right)B_1+\left(R_{sm}-R_m\right)B_2-\left(\hat{S}+\hat{d}^2\right)\tau\tau_m\Delta-\left(\hat{T}+\hat{d}^2\right)=0$ where

$$B_1=\frac{3+\tau_m}{360}+\frac{A_1\hat{t}e^{-p}\left(b_2-4a_2\right)+A_2\hat{t}e^{-p}\left(4a_1-b_1\right)}{a_2b_1-a_1b_2},$$

$$B_2=\frac{A_1\left(a_3b_2-a_2b_3\right)+A_2\left(a_1b_3-a_3b_1\right)}{\left(a_2b_1-a_1b_2\right)}+A_3,$$

$$A_1=\frac{\left(1+\frac{2\tau_m}{5}\right)p\left(e^{-p}+p-1\right)}{24\hat{t}\hat{d}\beta^2e^{-p}}+\frac{\left(1+\frac{\tau_m}{2}\right)\hat{\mu}p^2}{6\hat{t}e^{-p}}+\frac{\left(1+\frac{2\tau_m}{3}\right)\hat{d}p\left(1-e^{-p}\right)}{2\hat{t}e^{-p}}$$

$$+\frac{\left(1+\tau_m\right)\hat{d}\left(1-pe^{-p}-e^{-p}\right)}{\hat{t}e^{-p}}+A_4,$$

$$A_4=\hat{d}^2\left(\frac{-2-p}{2}+\frac{\left(e^p-1\right)}{p}\right)+2\tau\hat{d}^2\left(\frac{-6-2p}{12}+\frac{\left(e^p-p-1\right)}{p^2}\right),$$

$$A_3=\frac{-\left(1+\frac{2}{5}\tau_m\right)}{24\hat{t}\hat{d}\beta^2}+\frac{\left(1+\frac{\tau_m}{2}\right)\hat{\mu}}{6\hat{t}}+\frac{\left(1+\frac{2}{3}\tau_m\right)\hat{d}}{2\hat{t}}+\frac{\left(1+\tau_m\right)\hat{d}}{2\hat{t}}+d^2\left(\frac{2+\tau}{12}\right),$$

$$A_2=\frac{\left(1+\frac{2}{5}\tau_m\right)p\left(-e^p-p+1\right)}{24\hat{t}\hat{d}\beta^2}+\frac{\left(1+\frac{\tau_m}{2}\right)\hat{\mu}p^2e^{-p}}{6\hat{t}}+\frac{\left(1+\frac{2}{3}\tau_m\right)\hat{d}p\left(1-e^{-p}\right)}{2\hat{t}}$$

$$+\frac{\left(1+\tau_m\right)\hat{d}\left(-1+p+e^{-p}\right)}{\hat{t}}+A_5,$$

$$A_5=\frac{d^2\left(-p\left(2+p\right)-\left(e^{-p}-1\right)\right)}{2p}+\frac{2\tau d^2\left(p^2\left(-6-2p\right)+12\left(e^{-p}+p-1\right)\right)}{12p^2},$$

and the constants $a_i^{'s}$ and $b_i^{'s}$ are defined previously.

4.5 Piecewise linear salinity profile with salting from below

For this case, following Currie [9], $h(z)=\begin{cases}\varepsilon^{-1}, & 0\le z\le\varepsilon\\ 0, & \varepsilon\le z\le 1\end{cases}$, $h_m(z_m)=\begin{cases}\varepsilon_m^{-1}, & 0\le z_m\le\varepsilon_m\\ 0, & \varepsilon_m\le z_m\le 1\end{cases}$ where ε is the solutal depth in the fluid layer and ε_m is the solutal depth in the porous layer. The critical Rayleigh number R_{c4} for this profile is obtained from (26) and is solved from the equation $\left(R_{c4}\hat{t}-R_s\hat{s}\right)B_1+\left(R_{sm}-R_m\right)B_2-\left(\hat{S}+\hat{d}^2\right)\tau\tau_m\Delta-\left(\hat{T}+\hat{d}^2\right)=0$ where

$$B_1=\frac{1+\tau_m\varepsilon^4}{120}+\frac{A_1\hat{t}e^{-p}\left(b_2-4a_2\right)+A_2\hat{t}e^{-p}\left(4a_1-b_1\right)}{a_2b_1-a_1b_2},$$

$$B_2=\frac{A_1\left(a_3b_2-a_2b_3\right)+A_2\left(a_1b_3-a_3b_1\right)}{\left(a_2b_1-a_1b_2\right)}+A_3,\quad A_1=\frac{\left(1+\tau_m\varepsilon^3\right)p\left(e^{-p}+p-1\right)}{24\hat{t}\hat{d}\beta^2e^{-p}}+$$

$$\frac{\left(1+\tau_m\varepsilon^2\right)\hat{\mu}p^2}{6\hat{t}e^{-p}}+\frac{\left(1+\tau_m\varepsilon\right)\hat{d}p\left(1-e^{-p}\right)}{2\hat{t}e^{-p}}+\frac{\left(1+\tau_m\right)\hat{d}^2\left(1-pe^{-p}-e^{-p}\right)}{\hat{t}e^{-p}}+A_4,$$

$$A_4=\hat{d}^2\left(-1-\frac{p}{2}+\frac{\left(e^p-1\right)}{p}+\tau\left(-1-\frac{p\varepsilon_m}{2}+\frac{e^{p\varepsilon_m}-1}{p\varepsilon_m}\right)\right),$$

$$A_2=\frac{\left(1+\tau_m\varepsilon^3\right)pe^{-p}\left(-e^p-p+1\right)}{24\hat{t}\hat{d}\beta^2}+\frac{\left(1+\tau_m\varepsilon\right)\hat{d}p\left(1-e^{-p}\right)}{2\hat{t}}+$$

$$\frac{\left(1+\tau_m\varepsilon^2\right)\hat{\mu}p^2e^{-p}}{6\hat{t}}+\frac{\left(1+\tau_m\right)\hat{d}^2\left(-1+p+e^{-p}\right)}{\hat{t}}+A_5,$$

$$A_5=d^2\left(-1+\frac{p}{2}-\frac{\left(e^{-p}-1\right)}{p}+\tau\left(-1+\frac{p\varepsilon_m}{2}-\frac{e^{-p\varepsilon_m}-1}{p\varepsilon_m}\right)\right),$$

$$A_3=\frac{-\left(1+\tau_m\varepsilon^3\right)}{24\hat{t}\hat{d}\beta^2}+\frac{\left(1+\tau_m\varepsilon^2\right)\hat{\mu}}{6\hat{t}}+\frac{\left(1+\tau_m\varepsilon\right)\hat{d}}{2\hat{t}}+\frac{\left(1+\tau_m\right)\hat{d}^2}{2\hat{t}}+d^2\left(\frac{1+\tau\varepsilon_m^2}{6}\right),$$

and the constants $a_i^{'s}$ and $b_i^{'s}$ are defined previously.

4.6 Piecewise linear salinity profile with desalting above

In this case, following Vidal and Acrivos [10],

$$h(z)=\begin{cases}0, & 0\le z\le(1-\varepsilon)\\ \varepsilon^{-1}, & (1-\varepsilon)\le z\le 1\end{cases},\quad h_m(z_m)=\begin{cases}0, & 0\le z_m\le(1-\varepsilon_m)\\ \varepsilon_m^{-1}, & (1-\varepsilon_m)\le z_m\le 1\end{cases}$$

where ε is the solutal depth in the fluid layer and ε_m is the solutal depth in the porous layer. The critical Rayleigh number R_{c5} for this profile is obtained from (26) and is solved from the equation

$$\left(R_{c5}\hat{t}-R_s\hat{s}\right)B_1+\left(R_{sm}-R_m\right)B_2-\left(\hat{S}+\hat{d}^2\right)\tau\tau_m\Delta-\left(\hat{T}+\hat{d}^2\right)=0$$

where

$$B_1=\frac{1+\frac{\tau_m}{\varepsilon}\left(1-\left(1-\varepsilon\right)^5\right)}{120}+\frac{A_1\hat{t}e^{-p}\left(b_2-4a_2\right)+A_2\hat{t}e^{-p}\left(4a_1-b_1\right)}{a_2b_1-a_1b_2},$$

$$B_2=\frac{A_1\left(a_3b_2-a_2b_3\right)+A_2\left(a_1b_3-a_3b_1\right)}{\left(a_2b_1-a_1b_2\right)}+A_3,$$

$$A_1=\frac{\left(1+\frac{\tau_m}{\varepsilon}\left(1-\left(1-\varepsilon\right)^4\right)\right)p\left(e^{-p}+p-1\right)}{24\hat{t}\hat{d}\beta^2e^{-p}}+\frac{\left(1+\frac{\tau_m}{\varepsilon}\left(1-\left(1-\varepsilon\right)^3\right)\right)\hat{\mu}p^2}{6\hat{t}e^{-p}}+$$

$$\frac{\left(1+\frac{\tau_m}{\varepsilon}\left(1-\left(1-\varepsilon\right)^2\right)\right)\hat{d}p\left(1-e^{-p}\right)}{2\hat{t}e^{-p}}+\frac{\left(1+\tau_m\right)\hat{d}^2\left(1-pe^{-p}-e^{-p}\right)}{\hat{t}e^{-p}}+$$

$$\hat{d}^2\left(\frac{-2-p}{2}+\frac{\left(e^p-1\right)}{p}\right)+\frac{\tau\hat{d}^2}{\varepsilon_m}\left(-\varepsilon_m+\frac{p\left(\left(1-\varepsilon_m\right)^2-1\right)}{2}+\frac{e^p-e^{p\left(1-\varepsilon_m\right)}}{p}\right),$$

$$A_2=\frac{\left(1+\frac{\tau_m}{\varepsilon}\left(1-\left(1-\varepsilon\right)^4\right)\right)pe^{-p}\left(-e^p-p+1\right)}{24\hat{t}\hat{d}\beta^2}+\frac{\left(1+\frac{\tau_m}{\varepsilon}\left(1-\left(1-\varepsilon\right)^3\right)\right)\hat{\mu}p^2e^{-p}}{6\hat{t}}$$

$$+\frac{\left(1+\frac{\tau_m}{\varepsilon}\left(1-\left(1-\varepsilon\right)^2\right)\right)\hat{d}p\left(1-e^{-p}\right)}{2\hat{t}}+\frac{\left(1+\tau_m\right)\hat{d}^2\left(-1+p+e^{-p}\right)}{\hat{t}}+$$

$$d^2\left(\frac{-2+p}{2}-\frac{\left(e^{-p}-1\right)}{p}\right)+\frac{d^2\tau}{\varepsilon_m}\left(-\varepsilon_m+\frac{p\left(1-\left(1-\varepsilon_m\right)^2\right)}{2}+\frac{-e^{-p}+e^{-p\left(1-\varepsilon_m\right)}}{p}\right)$$

$$A_3=\frac{-\left(1+\frac{\tau_m}{\varepsilon}\left(1-\left(1-\varepsilon\right)^4\right)\right)}{24\hat{t}\hat{d}\beta^2}+\frac{\left(1+\frac{\tau_m}{\varepsilon}\left(1-\left(1-\varepsilon\right)^3\right)\right)\hat{\mu}}{6\hat{t}}+\frac{\left(1+\frac{\tau_m}{\varepsilon}\left(1-\left(1-\varepsilon\right)^2\right)\right)\hat{d}}{2\hat{t}}$$

$$+\frac{\left(1+\tau_m\right)\hat{d}^2}{2\hat{t}}+d^2\left(\frac{1}{6}+\frac{\tau}{6\varepsilon_m}\left(1-\left(1-\varepsilon_m\right)^3\right)\right)$$

and the constants $a_i^{'s}$ and $b_i^{'s}$ are defined previously.

4.7 Step function salinity profile

Here for this profile the basic concentration/solute/salt drops suddenly by an amount ΔS at $z=\varepsilon$ and ΔS_m at $z_m=\varepsilon_m$ otherwise uniform. Accordingly,

$h\left(z\right)=\delta\left(z-\varepsilon\right),\quad h_m\left(z_m\right)=\delta\left(z_m-\varepsilon_m\right)$ where ε is the solutal depth in the fluid layer and ε_m is the solutal depth in the porous layer. The critical Rayleigh number R_{c6} for this profile is obtained from (26) and is solved from the equation $\left(R_{c6}\hat{t}-R_s\hat{s}\right)B_1+\left(R_{sm}-R_m\right)B_2-\left(\hat{S}+\hat{d}^2\right)\tau\tau_m\Delta-\left(\hat{T}+\hat{d}^2\right)=0$ Where

$$B_1 = \frac{1+5\tau_m\varepsilon^4}{120} + \frac{A_1\hat{t}e^{-p}\left(b_2-4a_2\right)+A_2\hat{t}e^{-p}\left(4a_1-b_1\right)}{a_2b_1-a_1b_2},$$

$$B_2 = \frac{A_1\left(a_3b_2-a_2b_3\right)+A_2\left(a_1b_3-a_3b_1\right)}{\left(a_2b_1-a_1b_2\right)} + A_3$$

$$A_1 = \frac{\left(1+4\tau_m\varepsilon^3\right)p\left(e^{-p}+p-1\right)}{24\hat{t}\hat{d}\beta^2e^{-p}} + \frac{\left(1+3\tau_m\varepsilon^2\right)\hat{\mu}p^2}{6\hat{t}e^{-p}} + \frac{\left(1+2\tau_m\varepsilon\right)\hat{d}p\left(1-e^{-p}\right)}{2\hat{t}e^{-p}}$$

$$+\frac{\left(1+\tau_m\right)\hat{d}\left(1-pe^{-p}-e^{-p}\right)}{\hat{t}e^{-p}} + \frac{\hat{d}^2\left(-2-p\right)}{2} + \frac{\hat{d}^2\left(e^p-1\right)}{p} + \tau\hat{d}^2\left(-1-p+e^{p\varepsilon_m}\right),$$

$$A_2 = \frac{\left(1+4\tau_m\varepsilon^3\right)pe^{-p}\left(-e^p-p+1\right)}{24\hat{t}\hat{d}\beta^2} + \frac{\left(1+3\tau_m\varepsilon^2\right)\hat{\mu}p^2e^{-p}}{6\hat{t}} +$$

$$\frac{\left(1+2\tau_m\varepsilon\right)\hat{d}p\left(1-e^{-p}\right)}{2\hat{t}} + \frac{\left(1+\tau_m\right)\hat{d}^2\left(-1+p+e^{-p}\right)}{\hat{t}} +$$

$$\frac{d^2\left(-1+p\right)}{2} - \frac{d^2\left(e^p-1\right)}{p} + \tau d^2\left(-1+p+e^{-p\varepsilon_m}\right),$$

$$A_3 = \frac{-\left(1+4\tau_m\varepsilon^3\right)}{24\hat{t}\hat{d}\beta^2} + \frac{\left(1+3\tau_m\varepsilon^2\right)\hat{\mu}}{6\hat{t}} + \frac{\left(1+2\tau_m\varepsilon\right)\hat{d}}{2\hat{t}} + \frac{\left(1+\tau_m\right)\hat{d}^2}{2\hat{t}} + d^2\left(\frac{1}{6}+\frac{\tau\varepsilon_m^2}{2}\right)$$

and the constants $a_i^{'s}$ and $b_i^{'s}$ are defined previously.

5. RESULTS AND DISCUSSIONS

5.1 For linear, parabolic and inverted parabolic salinity profiles

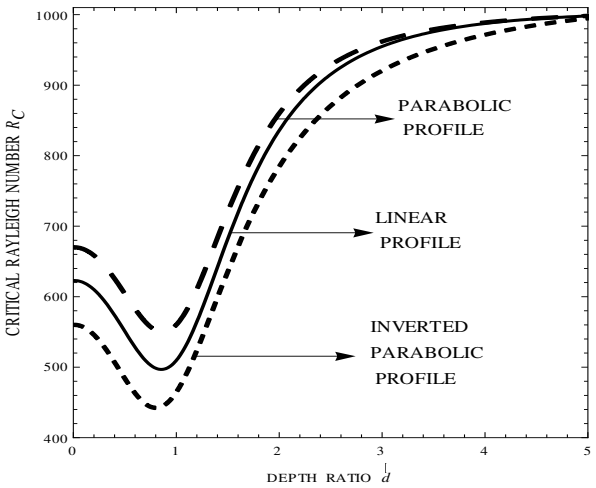

Figure-1. Variation of critical Rayleigh number R_c for linear, parabolic and inverted parabolic profiles with respect to depth ratio $\hat{d}$.

Figure-1 shows the variation of critical Rayleigh number R_c for Linear, Parabolic and Inverted Parabolic profiles with respect to depth ratio $\hat{d}$ for fixed values of $Da = 0.001,\ \hat{S} = 1,\ \hat{T} = 1,\ \tau_{pm} = 0.75,\ \tau = 0.5,\ R_s = 1000,\ \mu = 2.5,\ \hat{\kappa} = 1.$ The critical thermal Rayleigh number R_c for the profiles differ only for values of depth ratio $0 \le \hat{d} \le 5$. Graphically it is evident that the parabolic salinity profile is the most stable one and the inverted parabolic salinity profile is the unstable one, so by choosing the appropriate salinity profile one can control the onset of double diffusive convection in a composite layer.

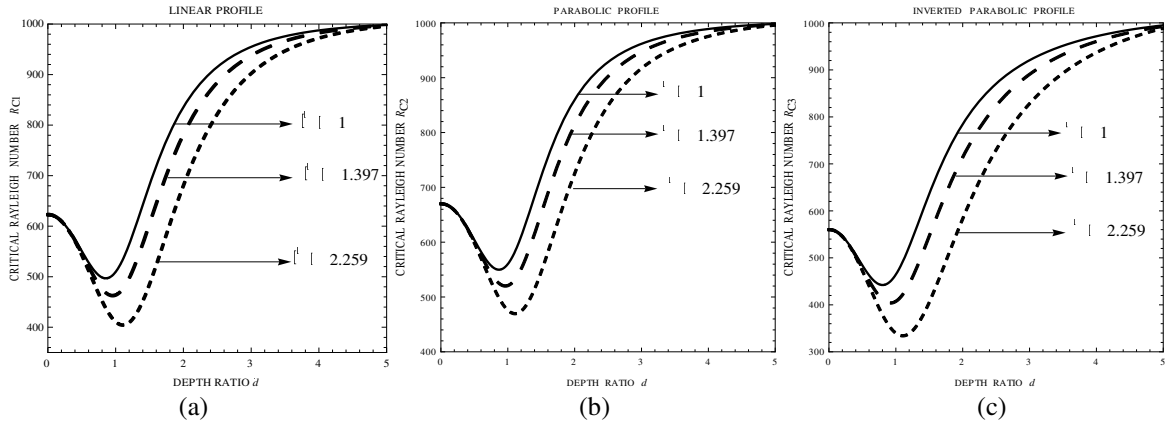

Figure-2. Effects of the thermal diffusivity ratio $\hat{\kappa}$ in linear, parabolic and inverted parabolic profiles on the critical thermal Rayleigh number R_{c1}, R_{c2} and R_{c3}.

The effects of the thermal diffusivity ratio $\hat{\kappa} = 1,\ 1.397,\ 2.259$, are displayed in Figures 2 (a), (b) and (c) respectively for fixed values of $Da = 0.001,\ \hat{S} = 1,\ \hat{T} = 1,\ \tau = 0.5,\ \tau_{pm} = 0.75,\ R_s = 1000,\ \hat{\mu} = 2.5,\ \varepsilon_m = 1.$. The curves in all the profiles are converging at both the ends that is, we can see the effect of the thermal diffusivity ratio $\hat{\kappa}$ only for the values of depth ratio $0.5 \le \hat{d} \le 5$, so the effect of the thermal diffusivity is limited to this range of depth ratio. In this range, for a fixed value of depth ratio, the increase in the value of $\hat{\kappa}$ decreases the critical

Thermal Rayleigh number. So thus destabilizes the system and hence the onset of the double diffusive convection is earlier.

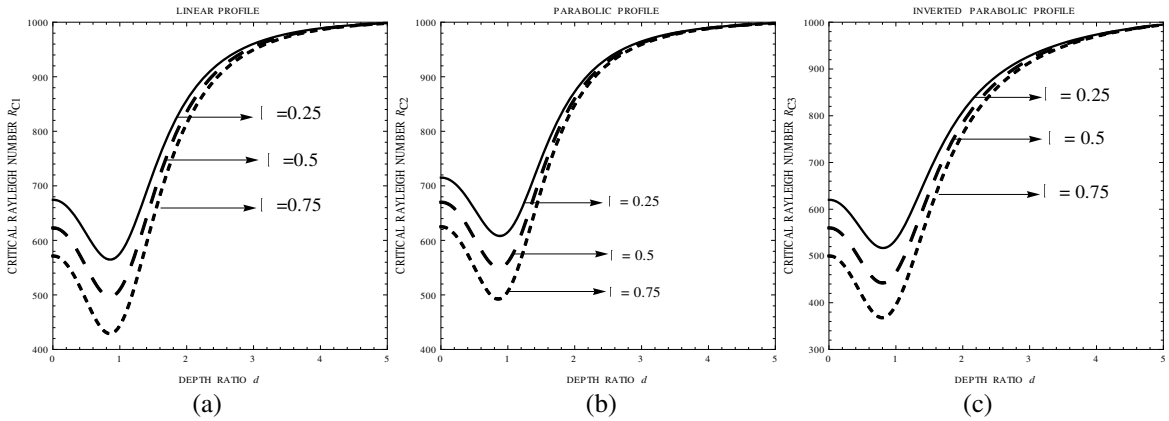

Figure-3. Effects of τ in linear, parabolic and inverted parabolic profiles on the critical thermal Rayleigh number R_{c1}, R_{c2} and R_{c3}.

The effects of the diffusivity ratio $\tau = \frac{\kappa_s}{\kappa}$, which is the solutal to thermal diffusivity ratio of the fluid in the fluid layer, are displayed in Figures 5(a), (b) and (c) for linear, parabolic and inverted parabolic salinity profiles respectively for fixed values of $Da = 0.001,\ \hat{S} = 1,\ \hat{T} = 1,\ R_s = 1000,\ \tau_{pm} = 0.75,\ \hat{\kappa} = 1,\ \hat{\mu} = 2.5,\ \varepsilon_m = 1$ .The curves in all the profiles are converging as the depth ratio increases, that is, the effect of the diffusivity ratio is only up to the depth ratio $\hat{d} = 3$.For a fixed value of $\hat{d}$ the increase in the values of τ ,decreases the value of the Thermal Rayleigh number R_c.Thus destabilizes the system and hence the onset of the double diffusive convection is quicker. Thus the system can be stabilized by decreasing this ratio that is, increasing the thermal diffusivity of the fluid layer or by decreasing the solute diffusivity of the fluid in the fluid layer.

5.2 For salting below, desalting above and step function salinity profiles

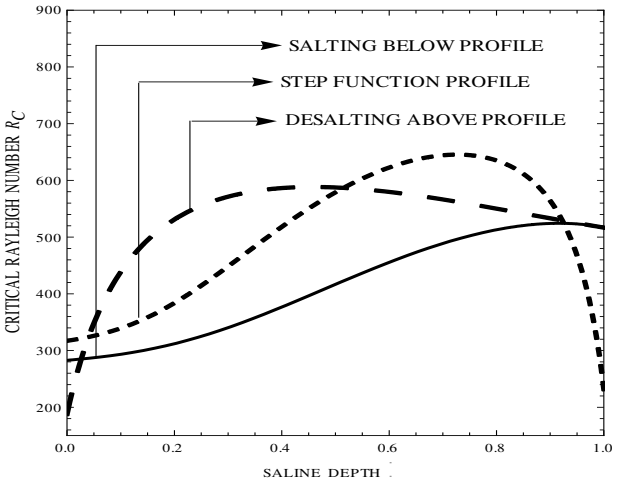

Figure-4. The variation of critical Rayleigh number R_c for salting below, desalting above and step function profiles with respect to the saline depth ε.

Figure-6 displays the variation of critical thermal Rayleigh number R_c for Salting below, Desalting above and Step function salinity profiles with respect to the saline depth ε for fixed values of $Da = 0.001,\ \hat{S} = 1,\ \hat{T} = 1,\ \tau = 0.5,\ \tau_{pm} = 0.75,\ R_s = 1000,\ \hat{\mu} = 2.5,\ \hat{\kappa} = 1,\ \varepsilon_m = 1.$ From the above graph it is clear that, step function salinity profile is stable for the solutal depth $0 \le \varepsilon \le 0.05$ and $0.5 \le \varepsilon \le 0.9$. Desalting above profile is stable for the solutal depth $0.05 \le \varepsilon \le 0.5$ and for the solutal depth $0.9 \le \varepsilon \le 1$ salting below and desalting above salinity profiles are stable also desalting above salinity profile is unstable for the solutal depth $0 \le \varepsilon \le 0.05$, salting below profile is unstable for the solutal depth $0.05 \le \varepsilon \le 0.9$ and for the solutal depth $0.9 \le \varepsilon \le 1$ step function salinity profiles is unstable. Thus we choose appropriate salinity profile to control the onset of double

diffusive convection in a composite layer. It can be understood easily from the following table.

Table-1. Salinity profile to control the onset of double diffusive convection.

Solutal depth ε	Stable profile	Unstable profile
$0 \le \varepsilon \le 0.05$	Step function salinity profile	Desalting above salinity profile
$0.05 \le \varepsilon \le 0.5$	Desalting above salinity profile	Salting below salinity profile
$0.5 \le \varepsilon \le 0.9$	Step function salinity profile	Salting below salinity profile
$0.9 \le \varepsilon \le 1$	Salting and desalting salinity profile	Step function salinity profile

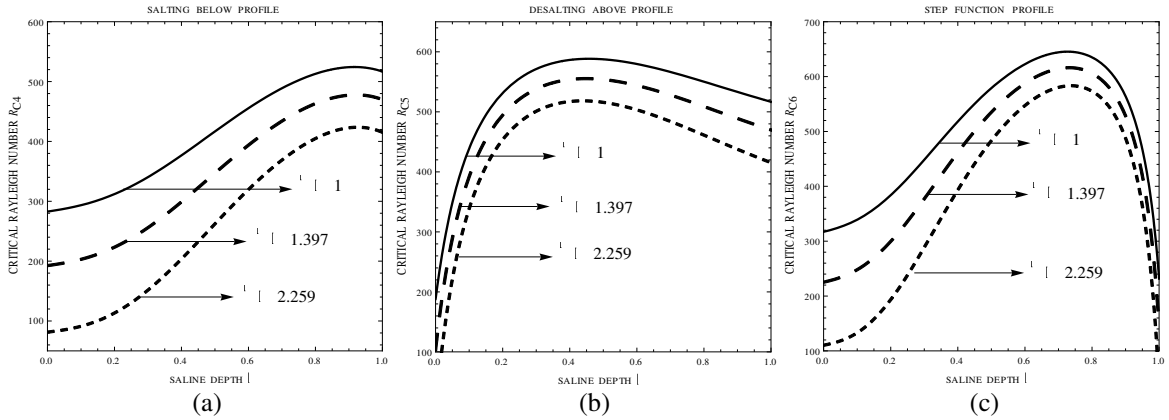

Figure-5. Effect of thermal diffusivity ratio $\hat{\kappa}$ in salting below, desalting above and step function profiles on the critical thermal Rayleigh number R_{c4}, R_{c5} and R_{c6}.

The effects of the thermal diffusivity ratio $\hat{\kappa} = 1, 1.397, 2.259$, are displayed in Figures 5(a), (b) and (c) respectively for fixed values of $Da = 0.001,\ \hat{S} = 1,\ \hat{T} = 1,\ \tau = 0.5,\ \tau_{pm} = 0.75,\ R_s = 1000,\ \hat{\mu} = 2.5,\ \varepsilon_m = 1.$ The curves are diverging in desalting above profile where the curves are converging for salting below and step function salinity profiles. For a fixed value of ε, with the increase in the value of $\hat{\kappa}$ the critical Thermal Rayleigh number decreases. This destabilizes the system and hence the onset of the double diffusive convection is rapidly.

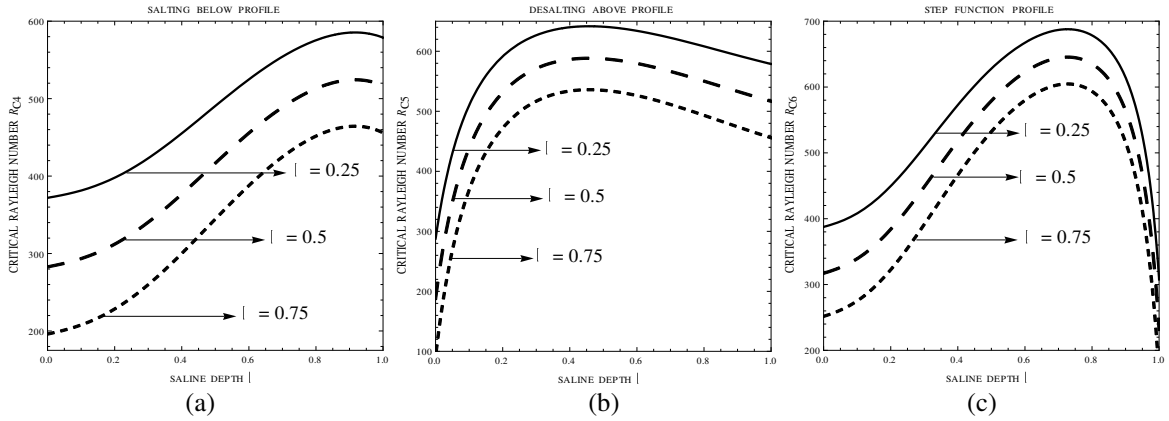

Figure-6. The effects of $\tau = 0.25,\ 0.5,\ 0.75$ in salting below, desalting above and step function profiles on the critical thermal Rayleigh number R_{c4}, R_{c5} and R_{c6}.

The effects of the diffusivity ratio $\tau = \dfrac{\kappa_S}{\kappa}$, which is the ratio of saline to thermal diffusivity of the fluid are displayed in Figures 6 (a), (b) and (c) respectively for fixed values of $Da = 0.001,\ \hat{S} = 1,\ \hat{T} = 1,\ \hat{\mu} = 2.5,\ \tau_{pm} = 0.75,\ R_s = 1000,\ \hat{\kappa} = 1,\ \varepsilon_m = 1.$ The curves in desalting above are diverging i.e., the effect is more for greater values of solutal depth ε and it is reverse for Step function salinity profile.From the graph it

can be seen that with the increase in the value of τ decreases the critical Thermal Rayleigh number R_c. Thus destabilizes the system and hence the onset of the double diffusive convection is earlier.

6. CONCLUSIONS

a) For the stability demanding situations like solar ponds, the parabolic salinity profile is the most conducive where in the onset of double diffusive convection in a composite layer can be deferred.

b) For the heat and mass (solute or salt) transfer problems like petroleum and geothermal reservoirs, the inverted parabolic salinity profile is most suitable, where in the onset of double diffusive convection can be quicker.

c) Increasing the parameters viscosity ratio and solute Rayleigh number and decreasing the parameters thermal diffusivity ratio and the solute to thermal diffusivity ratio the onset of double diffusive convection in a composite layer can be delayed for all the salinity profiles.

ACKNOWLEDGEMENT

We express our gratitude to Prof. N. Rudraiah and Prof. I.S. Shivakumara, UGC-CAS in Fluid mechanics, Bangalore University, Bangalore, for their help during the formulation of the problem.

REFERENCES

[1] Subbarama Pranesh, Arun Kumar and Narayanappa. 2012. Effect of Non Uniform Basic Concentration Gradient on the Onset of Double Diffusive Convection in Micropolar Fluid. Scientific Research an academic publisher. 3(5).

[2] Ray-Yeng Yang, Hwung Hweng Hwung and Igor V. Shugan. 2009. Over stability analysis on salt fingers convection with parabolic temperature and salinity profiles, Acta Astronautica. 65(1): 240-247.

[3] Margarida Giestas, Heitor L. Pina, Jorge Milhazes and Clia Tavares. 2009. Solar pond modeling with density and viscosity dependent on tem- perature and salinity. International Journal of Heat and Mass Transfer. 52. 28492857.

[4] Chen F and Chen C. F. 1988. Onset of Finger Convection in a horizontal porous layer underlying a fluid layer, J. Heat transfer. 110, 403.

[5] Nield D A. 1977. Onset of convection in a fluid layer overlying a layer of a porous medium. J. Fluid Mech. 81, 513.

[6] Venkatachalappa M, Prasad Shivakumara I S. and Sumithra R 1997. Hy- drothermal growth due to double diffusive convection in composite materi- als. Proceedings of 14th National Heat and Mass Transfer Conference and 3rd ISHMT ASME Joint Heat and Mass transfer conference, December 29-31.

[7] Shivakumara I.S, Suma Krishna B. 2006. Onset of surface tension driven con - vection in superposed layers of fluid and saturated porous medium, Arch. Mech. 58, 2, pp.71-92, Warszawa.

[8] Sparrow E M, Goldstein R J and Jonsson V K. 1964. Thermal instability in a horizontal fluid Lauer: Effect of boundary conditions and non linear temperature profile. J. Fluid Mechanics. 18, 513.

[9] Currie I G. 1967. Isotropic composition and origin of the Red sea and Salton Sea geothermal brines, science. 154, 1544.

[10] Vidal A and Acrivos A. 1966. Nature of the neutral state in surface tension driven convection, Phys. Fluids. 9, 615.